HAL
open science

DNA-PK promotes the survival of young neurons in the embryonic mouse retina.

Enrique J de La Rosa, Jimena Baleriola, Teresa Suárez

To cite this version:

Enrique J de La Rosa, Jimena Baleriola, Teresa Suárez. DNA-PK promotes the survival of young neurons in the embryonic mouse retina.. Cell Death and Differentiation, 2010, 10.1038/cdd.2010.46 . hal-00533511

HAL Id: hal-00533511

https://hal.science/hal-00533511v1

Submitted on 7 Nov 2010

HAL is a multi-disciplinary open access archive for the deposit and dissemination of scientific research documents, whether they are published or not. The documents may come from teaching and research institutions in France or abroad, or from public or private research centers.

L'archive ouverte pluridisciplinaire **HAL**, est destinée au dépôt et à la diffusion de documents scientifiques de niveau recherche, publiés ou non, émanant des établissements d'enseignement et de recherche français ou étrangers, des laboratoires publics ou privés.

Title: DNA-PK promotes the survival of young neurons in the embryonic mouse retina

Running title: DNA damage and repair in neurogenesis

Authors: Jimena Baleriola, Teresa Suárez and Enrique J. de la Rosa

Affiliation: 3D Lab (Development, Differentiation & Degeneration), Department of Cellular and Molecular Medicine, Centro de Investigaciones Biológicas, Consejo Superior de Investigaciones Científicas, Spain

Corresponding author: Enrique J. de la Rosa, CIB-CSIC, C/ Ramiro de Maetzu 9, E-28040 Madrid, Spain. Phone: 34-918373112, ext 4375. Fax: 34-915360432. E-mail: ejdelarosa@cib.csic.es

Abstract

Programmed cell death is a crucial process in neural development that affects mature neurons and glial cells, as well as proliferating precursors and recently born neurons at earlier stages. However, the regulation of the early phase of neural cell death and its function remain relatively poorly understood. In mouse models defective in homologous recombination (HR) or non-homologous end-joining (NHEJ), which are both DNA double-strand break (DSB) repair pathways, there is massive cell death during neural development, even leading to embryonic lethality. These observations suggest that natural DSBs occur frequently in the developing nervous system. Here we have found that several components of DSB repair pathways are activated in the developing mouse retina at stages that coincide with the onset of neurogenesis. In short-term organotypic retinal cultures, we confirmed that the repair pathways can be modulated pharmacologically. Indeed, inhibiting DNA-PKcs, which is involved in NHEJ, with NU7026 increased caspase-dependent cell death and selectively reduced the neuron population. This observation concurs with an increase in the number of apoptotic neurons found after NU7026 treatment, as also observed in the embryonic *scid* mouse retina, a mutant that lacks DNA-PKcs activity. Therefore, our results implicate the generation of DSB and DNA-PK-mediated repair in neurogenesis in the developing retina.

Keywords: Double-strand break, DNA repair, non-homologous end-joining, retinal ganglion cell, apoptosis, programmed cell death, neuronal differentiation.

Abbreviations: ATM, Ataxia Telangiectasia Mutated; ATR, Ataxia Talangiectasia and Rad-3 Related; DNA-PK, DNA-Dependent Protein Kinase; DNA-PKcs, DNA-PK

catalytic subunit; DSB, Double-Strand Break; E, embryonic day; γH2AX, Ser^{139} phosphorylated histone H2AX; HR, Homologous recombination; NHEJ, Non-Homologous End-Joining; P, postnatal day; RGC, Retinal Ganglion Cell; RT, room temperature; SCID, Severe Combined Immune Deficiency; TUNEL, TdT-mediated dUTP nick end-labeling.

Introduction

During neural development, programmed cell death occurs from the early stages of proliferation until the later stages of functional maturation, constituting part of the process generating the sophisticated cytoarchitecture and connectivity of the nervous system. Although the early phase of cell death affecting proliferating neuroepithelial cells and recently born neurons has been recognized, how it is regulated and its function have only partially been characterized.[1-3] The relevance of early neural cell death has become evident in genetically modified mice, which also provide some clues as to the elements that control its regulation and function.[1-4] Besides the strong reduction in cell death found in knock-out mice deficient in executor and regulatory pro-apoptotic genes, a dramatic increase in neural cell death has been observed in animals with deficient DSB repair. Since most other tissues are only weakly affected or they are not affected at all, it appears that DSBs are selectively generated during neural development and that they underlie the early phase of cell death occurring in this tissue.[2, 5-10]

DSBs, the most deleterious kind of alteration to DNA, are produced by endogenous or exogenous agents. During normal embryonic development, DSBs are likely to be a consequence of endogenous cellular activity and they may be caused by replication stress during proliferation, transcriptional activity or oxidative stress produced by normal metabolism.[11, 12] In addition, DSBs can be programmed to generate diversity in the immune system.[13] In eukaryotes, DSBs are repaired by either HR or NHEJ. HR repairs DSBs without altering the DNA sequence, using a sister chromatid as an undamaged template. Conversely, NHEJ involves the direct ligation of the two DNA ends without ensuring that the correct sequence is restored. Thus, while HR is functionally important in the cell-cycle phases from synthesis to mitosis, NHEJ participates in repair throughout the cell-cycle and in post-mitotic cells. Although NHEJ

is an error-prone repair process, it is considered the predominant pathway in mammals.[7, 12]

DSBs trigger a signaling cascade that leads to the rapid formation of a repair focus at the break. One of the earliest events in the DNA damage response is the Ser^{139} phosphorylation of histone H2AX (γH2AX) by members of the phosphatidylinositol-3 kinase-like family, such as ATR, ATM and DNA-PK.[14] The presence of these activated proteins in foci implies a pre-existing DSB. Although these kinases share downstream substrates and cooperate under certain conditions, they have non-redundant functions.[12, 14, 15] Both ATR and ATM are checkpoint kinases that coordinate cell cycle progression after DNA damage. While ATR is activated by single-stranded overhangs generated at DSBs or single-stranded DNA originated from stalled replication forks during S phase, ATM responds to DSBs[15, 16] and it has been implicated in the NHEJ repair pathway.[17] DNA-PK is a protein complex required for efficient NHEJ, which includes Ku70, Ku80 and the DNA-PK catalytic subunit (DNA-PKcs).[7, 13]

The neuroretina is a classic model system to study basic cellular processes involved in neural development, including cell death.[18, 19] Retinas can be grown *ex vivo* in organotypic cultures with chemically defined medium, where proliferation, differentiation and cell death follow a developmental course similar to that seen *in vivo*.[20-22] Short-term pharmacological manipulations can be employed in these organotypic cultures to define the relationship and hierarchy between ongoing processes, which is not always possible in genetically manipulated animals due to the activation of compensatory events. We have inhibited ATM or DNA-PK activity in organotypic cultures of the mouse neuroretina at embryonic day (E) 14.5 to define the populations affected by DSBs and to characterize the selective contribution of DNA repair pathways to retinal development. Remarkably, diminished DNA-PK activity

resulted in selective death of recently born neurons, an observation corroborated in the embryonic retina of *scid* mice, thereby supporting a selective role for NHEJ in early retinal neurogenesis.

Results

Divergent patterns of cell death and H2AX activation in the developing mouse retina

To characterize the relationships between the generation and repair of DSBs, programmed cell death and neuronal differentiation, we studied several developmental stages between E13.5, when the generation of retinal ganglion cells (RGCs) has recently commenced, and postnatal day (P) 2, when a prominent phase of neurotrophic cell death affects RGCs (see refs. 18 and 19 for details). The presence of DSBs was determined by γH2AX immunostaining, whereas TdT-mediated dUTP nick end-labeling (TUNEL) was employed to visualize cell death (Figure 1). Cells undergoing each of these processes were evident in freshly dissected, whole-mount retinas at all the ages studied (Figure 1G), although the relative number of cells undergoing each process did not evolve in parallel. Whereas the density of TUNEL-positive cells was similar between E14.5 and P2, the density of γH2AX diminished after E16.5 and it reached a minimum at P2 (Figure 1, A-G). To corroborate the differential activation of H2AX between E14.5 and P2, freshly dissected retinas from both ages were dissociated into single cell suspensions and processed for γH2AX immunostaining to reveal discrete nuclear foci, a landmark of activated DSB repair (Figure 1, H-K). In close correlation with the observations from whole mount retinas, H2AX phosphorylation was greater at E14.5 than at P2 by considering both the percentage of cells with nuclear foci and the number of foci per cell. This observation confirmed that DSBs are more abundant at early stages of retinal development. The differential activation of H2AX was not accompanied by fluctuations in H2AX mRNA or in the expression of other molecules that respond to DNA damage (Supplementary Figure 1). Thus, unlike other model systems, [23] H2AX activation during retinal development does not appear to be linked to apoptotic DNA

cleavage but rather, to some other process occurring selectively at early developmental stages.

In the light of these results, we focused on E14.5 retinas when the γH2AX and TUNEL quantification were more similar than at later stages, and when both DSB repair and cell death co-exist with neuron generation, particularly that of RGCs. In order to establish a possible association between H2AX activation and cell death, we first compared the patterns of staining in whole mount retinas. Markers for both these processes were occasionally present in the same cell (Figure 2, A-B). Although γH2AX co-localized with TUNEL, it more frequently co-localized with Anexin-V staining (3-4 fold, data not shown), an earlier marker of programmed cell death than TUNEL. This preferential association of γH2AX with an early marker of apoptosis again indicated that H2AX activation is not a consequence of the apoptotic DNA cleavage revealed by TUNEL, at least during retinal development. In addition to γH2AX, additional landmarks of active DSB repair were found in discrete nuclear foci, namely Ser^{1981} phosphorylated ATM and DNA-PK, with some overlap in the distribution of pATM and γH2AX (Figure 2, C-F). Thus, the DSB repair machinery seems to be intrinsically active in the developing mouse retina.

DSB repair pathways can be modulated in E14.5 retinas *ex vivo*

Next, we established an experimental design to induce the activation of DSB DNA repair in the embryonic retina and to experimentally manipulate this process. The topoisomerase II inhibitor etoposide provokes DSBs, as well as the rapid activation of ATM, ATR, DNA-PK and their corresponding substrates.[24-26] Exposing E14.5 retinas to etoposide in organotypic culture increased the accumulation of γH2AX and total p53 (Figure 3A), two common substrates of ATM, ATR and DNA-PK[13, 14, 16], and indicative

of the response of retinal cells to a genotoxic agent. Chk1, which is primarily activated by ATR[16, 27], also appeared to be phosphorylated in etoposide-treated retinas. Further, the levels of p21, a protein that regulates cell cycle progression after DNA damage in a p53-dependent manner,[16, 28] were found increased after etoposide treatment (Figure 3A). At the cellular level, etoposide induced the appearance of a large number of γH2AX nuclear foci after 30 minutes. These foci progressively disappeared over a 150 minute period after the removal of etoposide, prior to the appearance of apoptotic cells in the tissue (Figure 3, B-F and data not shown). These results indicate that the developing retina could modulate the activation of the repair process in response to DNA damage.

Inhibition of DNA-PK *ex vivo* and its deficiency *in vivo* result in increased cell death in the E14.5 retina

In the light of our observation *in vivo* during retinal development, we focused on the NHEJ repair pathway, which is the only process capable of acting on young, post-mitotic neurons that are actively generated at E14.5. DNA-PK is an essential component of this pathway and it can be inhibited by NU7026. E14.5 retinas cultured in the presence of NU7026 had reduced levels of γH2AX and total p53, but not of pAkt, an important survival mediator that is also a downstream substrate of phosphatidylinositol-3 kinase activity (Figure 4, A and B). In etoposide-treated retinas, the selectivity of NU7026 treatment was compared with that of KU55933, an inhibitor of ATM. KU55933 reduced etoposide-mediated increase of p21, a downstream substrate of ATM, but not of pChk1, primarily activated by the related ATR kinase. Conversely, DNA-PK inhibition did not affect either of these substrates[16, 27, 28] (Figure 4C).

Having confirmed the selective inhibitory effects of NU7026 and KU55933, we studied the cellular consequences of interfering with the intrinsic activity of DNA-PK. It should

be noted that in these experiments, no treatment was used to exogenously induce DSBs and the repair pathways (i.e. UV irradiation or genotoxic agents), and the ATM inhibitor KU55933 was used as a control in selected experiments to better define the processes selectively dependent on DNA-PK. There was a significant increase in the density of TUNEL-positive nuclei in cultured E14.5 retinas after as little as 6 hours in the presence of NU7026 (Figure 5, A-D), whereas KU55933 did not induce cell death under similar conditions. As shown above (Figure 4, A and B), NU7026 did not affect Akt phosphorylation at the concentrations used, indicating that its effect on cell survival was not due to non-specific inhibition of the phosphatidylinositol-3 kinase-Akt survival pathway. To strengthen our observations, we analyzed the retinal phenotype of a mouse model with severe combined immunodeficiency (SCID) that expresses a truncated, enzymatically inactive form of DNA-PKcs.[29] While in E14.5 retinas no differences were found in the proportion of total γH2AX-positive cells, the γH2AX-staining pattern in *scid* retinas was imprecise (Supplementary figure 2). Some cells in *scid* retinas presented diffuse nuclear staining, while a reduced proportion had nuclear foci but fewer than the wild type, thus suggesting that the NHEJ repair process is disturbed in this animal. The retinas from *scid* mouse had a higher density of TUNEL-positive nuclei than the corresponding wild type retinas (Figure 5, E- G), which correlated well with our previous *ex vivo* findings.

In addition to our observations with TUNEL as a marker of programmed cell death, both the retinas exposed to NU7026 and those from the *scid* mouse had increased levels of activated caspase-3 (Figure 6), one of the main executors of apoptotic cell death in the developing nervous system.[2, 4, 30] Accordingly, the increase of TUNEL-positive nuclei in the presence of the DNA-PK inhibitor was prevented by the general caspase inhibitor Boc-D-fmk (Figure 6D). Both these *ex vivo* and *in vivo* results support the

involvement of DNA-PK, and likely of the NHEJ repair pathway, in regulating the correct levels of cell death in the developing retina. Hence, we further analyzed the impact of DNA-PK activity on other ongoing cellular processes.

Ex vivo inhibition of DNA-PK selectively affects neuronal number in the E14.5 retina

E14.5 retinas mostly contain proliferating neuroepithelial cells that can be identified by PCNA immunodetection, through the incorporation of BrdU, or by pH3 immunodetection when they undergo mitosis (Supplementary figure 3). However, none of these markers were significantly affected when retinas were exposed to the DNA-PK inhibitor NU7026 (Supplementary figure 3). Neurons, mainly RGCs, are actively generated at E14.5 and they are affected by the early phase of programmed cell death.[18-19] The population of neurons identified by βIII tubulin immunostaining was significantly reduced by NU7026 (Figure 7, A and B). Additional neuronal markers were employed in immunoblots. The expression of Islet was also significantly reduced after DNA-PK inhibition (Figure 7, D and E). Brn3a levels were also reduced to a similar extent, although the variability limited the significance of this observation. Interestingly, the general caspase inhibitor Boc-D-fmk prevented the loss of these neuronal markers in all cases (Figure 7, C, D and F).

Contrary to our observations in cultured retinas, we did not detect any reduction in these neuronal markers in the retinas from *scid* mice (Figure 7, H and I), possibly due to compensatory changes. This observation, which may lead to the underestimation of the real impact of the generation and repair DSBs during neurogenesis, encouraged us to carry out a more detailed characterization of the dying cells observed *ex vivo* and *in vivo* after interference with DNA-PK.

Inhibition *ex vivo* and *in vivo* deficiency of DNA-PK induced neuronal cell death in the E14.5 retina

To establish a direct relationship between the reduced number of neurons and the increase in programmed cell death, the density of Islet-positive neurons stained for apoptotic markers was assessed in both the NU7026-treated and the *scid* mouse retinas (Figure 8). In agreement with our earlier results (Figure 5D), the density of TUNEL-positive, Islet-positive nuclei increased in cultured wild-type E14.5 retinas after DNA-PK inhibition, but not after the inhibition of ATM (Figure 8, A-D). When activated-caspase 3 was employed as an alternative apoptotic marker, no significant differences were observed (data not shown), perhaps due to the small number of activated-caspase 3-positive cells present in the retina (fewer than the cells identified by TUNEL: see Figures 5, D and G for TUNEL, and 6, C and G for activated-caspase 3). However, an alternative method to visualize cells with general caspase activity again demonstrated increased numbers of Islet-positive, caspase-active cells in the presence of NU7026 (Figure 8, E-G). Through this approach, we also found an increase in the numbers of apoptotic Islet-positive young neurons in *scid* mouse retinas with respect to the corresponding wild type (Figure 8, H-M). This increase was even greater when cell death was determined by TUNEL. Hence, our results indicate that young neurons at early stages of retinal development require correct DNA-PK activity for survival.

Discussion

Our results show that, under physiological conditions, the embryonic mouse neuroretina expresses several markers that reveal the existence of DSBs as well as of active DNA repair. This expression overlaps with developmental processes, namely neuroepithelial cell proliferation, neuron generation and the early phase of programmed cell death. Pharmacological inhibition of intrinsic DNA-PK activity with NU7026 in E14.5 neuroretina organotypic cultures, in the absence of any additional treatment to induce DNA damage, increased caspase-dependent cell death and selectively reduced the population of young neurons. Whereas the initial observation was confirmed in the embryonic retina of *scid* mice that lack DNA-PK activity, no reduction of neuronal markers was found *in vivo*. However, an increased number of Islet-positive neurons double-labeled with apoptotic markers were found in both, NU7026-treated and *scid* mouse retinas, supporting the requirement of intrinsic DNA-PK activity for the survival of recently differentiated neurons, likely RGCs.

We previously employed retinal organotypic cultures to characterize an early phase of programmed cell death in the embryonic chick and mouse retina that was further corroborated *in vivo*.[20-22, 31] This process had been overlooked due to the high plasticity and the rapid pace of early development. Here we employ again short term pharmacological treatments in organotypic cultures, a type of culture that maintains a physiological environment and reproduces the early developmental processes fairly well, to establish the relationship between DSB repair, cell death, and the affected cell types, which are essential aspects that may be partially masked by redundancy and compensatory changes in knock-out animals. In our hands, E14.5 retinal organotypic cultures responded to the genotoxic stimulus of etoposide in just 30 minutes, by forming a large number of γH2AX-positive nuclear foci that disappeared more slowly upon

etoposide removal. Furthermore, this treatment upregulated several substrates of ATM, ATR and DNA-PK that participate in DSB repair and cell cycle progression. These substrates were selectively downregulated in the presence of pharmacological inhibitors, showing the ability of the developing retina to respond to DNA damage *ex vivo*.

We took advantage of the fact that several markers of an active DNA repair process were naturally present in the E14.5 mouse retina in order to establish the short-term consequences of interfering with the physiologically activated DNA repair process, without any additional extrinsic stimuli. Selective inhibition of DNA-PK, but not of ATM, increased caspase-dependent cell death, an observation that correlates well with the phenotype of mutant mice.[16, 29, 32] Further, interference with DNA-PK reduced the number of young neurons, without producing a clear effect on proliferating cells, and this effect was reverted by a pan-caspase inhibitor. DNA-PK inhibition directly affected neuronal survival. Indeed, the number of Islet-positive neurons displaying apoptotic markers increased in the presence of the DNA-PK inhibitor, but not in the presence of an ATM inhibitor, supporting a specific role for DNA-PK in neuronal survival at this particular developmental stage. The lack of response of retinal neurons to ATM inhibition was unexpected. ATM has been described to be involved in neuronal apoptosis at later stages[33]. The role of ATM in retinal neurogenesis deserves future studies.

The selective involvement of the DSB repair pathways in neural development is also evident in genetically modified animals. For instance, HR deficiency caused by the deletion of the *Brca1* or *Xrcc2* genes provokes embryonic lethality in mice due to increased apoptosis and decreased proliferation. Several regions of the nervous system are affected in these animal models, and while the *Brca1* knockout mice develop exencephaly and spina bifida,[9] the loss of *Xrcc2* affects the forebrain and the

hindbrain.[7, 10] *Xrcc4* and *LigIV* are involved in NHEJ and their absence in mice leads to death at about E14.5 due to large-scale apoptosis affecting early post-mitotic neurons.[5, 7, 8] Therefore, although HR and NHEJ repair pathways are able to cooperate in proliferating systems, in the developing nervous system they seem to act selectively and separately in neural cells depending on their developmental stage, an observation that concurs with our *ex vivo* results.

The physiological relevance of our findings has been verified in the E14.5 retina from *scid* mice. Most of the phenotypes found *ex vivo* in the retinas treated with NU7026 were also observed in this mouse model, particularly the caspase-dependent cell death affecting young neurons. Interestingly and supporting our combined approach, retinas treated with NU7026 for only six hours showed a downregulation of neuronal markers coincident with the increase of neuronal death, which we favor as the primary DNA-PK inhibition phenotype. This reduction in neuronal markers was not clear in the retina of *scid* embryos, probably due to compensatory effects.

Several key questions that remain pending are related to DSB generation. The accumulation of DSBs may be the result of DNA replication, transcription or oxidative metabolism, as postulated to explain the impact of deficient DSB repair in development.[11, 12, 32] However, these alternatives do not explain the selectivity of the tissues and cells affected, the immune and nervous systems, [2, 6] and more specifically the effects on young neurons in both the knock-out animals and through our pharmacological approach.[5, 7, 8, 11] One might speculate that in the central nervous system, as in the immune system, DSBs underlie genomic re-arrangements that trigger apoptosis if not adequately repaired. Events similar to somatic recombination have not been demonstrated in the central nervous system. Nevertheless, LINE-1-mediated retrotransposition, an additional source of DSBs that also activates the DNA damage

response, seems to be associated with neural differentiation in both rat and human neural progenitors, giving rise to somatic mosaicism.[34, 35] Intriguingly, the human hippocampus and other brain regions contain 1,000 times more endogenous copies of LINE-1 than the heart or the liver.[36] LINE-1-mediated retrotransposition during neurogenesis and the consequent error-prone NHEJ repair process may underlie the early phase of neural cell death, which is magnified in DSB repair deficient mice, as well as our present observations.

Short-term *ex vivo* pharmacological approaches may serve to further analyze the role of alternative DSB repair pathways independently. More important, they could be used to uncover phenotypes that are not always evident when embryos are analyzed. In addition, they could be combined with more detailed analyses of the knock-out mice available to provide further evidence of the relationships between DSB generation and neural development.

Materials and methods

Mice

C57BL/6J, BALB/c and *Prkdc*^{scid}/*Prkdc*^{scid} mice were reared in local facilities under a 12-h light:12-h dark cycle at 20°C. Mice were mated and the morning of appearance of a vaginal plug was designated E0.5. Mouse embryos were collected from euthanized pregnant females, while other experiments were carried out on postnatal mice at day 2. Unless indicated, all experiments were performed on C57Bl/6 embryos and postnatal animals. All experiments were approved by the local ethics committee for animal experiments and they were carried out in accordance with the European Union guidelines.

Genotyping of embryos carrying the *Prkdc*^{scid} mutation was performed as previously described [37].

Neuroretina organotypic culture

Eyes were collected from E14.5 embryos and the neuroretina was dissected free of surrounding tissues. Isolated neuroretinas were plated in chemically defined DMEM/F12 (GibcoBRL, New York, NY, USA) with N2 supplement (Sigma, St Louis, MI, USA) and cultured for 6 h at 37°C in 5% CO_2. Where indicated, etoposide (10 μM, Sigma), NU7026 (200 nM, Calbiochem, Darmstadt, Germany), KU99533 (13 nM, Tocris Bioscience, Bristol, UK), Boc-D-fmk (38 μM, Calbiochem) or BrdU (5 μM, Sigma) were added to the medium. After culture, the retinas were washed twice with phosphate-buffered saline (PBS) and processed as required.

Detection of apoptosis

TdT-mediated dUTP nick end-labeling of fragmented DNA was performed using FITC-dUTP on E13.5 to P2 whole-mount retinas as described previously[21] and according to

the manufacturer's instructions (Apoptosis Detection System; Promega, Madison, WI, USA). Briefly, freshly dissected or cultured retinas were flat-mounted onto nitrocellulose membranes and fixed overnight in 4% paraformaldehyde (w/v) in 0.1 M phosphate buffer (pH 7.4) at 4°C. Fixed neuroretinas were permeated for 2 h with 1-4% Triton X-100 (w/v; Fluka, Buchs, Switzerland), depending on the developmental stage, mildly digested for 10 min at 37°C with proteinase K (20 μg/ml, Promega) and fixed again with 4% paraformaldehyde (w/v) in 0.1 M phosphate buffer (pH 7.4) for 20 min at room temperature (RT). After several washes with PBS, the retinas were stained by TUNEL, mounted with Vectashield mounting medium (Vector Laboratories, Burlingame, CA, USA) and analyzed by confocal microscopy (Leica TCS-SP2-A0BS, Leica Microsystems GmbH, Wetzlar, Germany). The density of the apoptotic bodies was determined by counting TUNEL-positive nuclei and nuclear fragments throughout the whole retina with a 40X objective on a Zeiss fluorescence microscope (Zeiss Axioplan, Oberkochen, Germany).

For Annexin-V staining (TACS™ Annexin V-Biotin Apoptosis Detection Kit; Trevigen, Gaithersburg, MD, USA), freshly dissected E14.5 retinas were flat-mounted onto nitrocellulose membranes and incubated for 30 minutes at 37°C and 5% CO_2 with 4% Annexin-V-biotin and 5% binding buffer in culture medium. After several washes with PBS, the retinas were fixed 3 h with 4% paraformaldehyde at RT and permeated as described above. The retinas were further incubated for 1 h with Alexa-488 conjugated to avidin (Molecular Probes, Invitrogen, Carlsbad, CA, USA), washed with PBS, mounted with Vectashield mounting medium and analyzed by confocal microscopy.

In situ caspase activity labeling was performed in E14.5 retinas using the CaspACE™ FITC-VAD-fmk Marker (Promega). 10 μM FITC-VAD-fmk was directly added to the organotypic retinal cultures, during the last hour of incubation. The retinas were then

washed several times with PBS, flat-mounted onto nitrocellulose membranes and fixed 3 h at RT with 4% paraformaldehyde. Fixed neuroretinas were mounted with Vectashield mounting medium and analyzed by confocal microscopy. Cells stained for activated caspases were scored throughout the whole retina with a 100X objective on a Zeiss Axioplan fluorescence microscope.

Immunostaining of whole-mount retinas

Freshly dissected or cultured retinas were flat-mounted, fixed and permeated as above. The retinas were subsequently incubated overnight at 4ºC with primary antibodies against activated caspase-3 (1/100, Cell Signaling Technology, Danvers, MA, USA); γH2AX (1/1000, Abcam, Cambridge, UK); pH3 (Ser^{10}, 1/100, Millipore, Billerica, MA, USA); or Islet-1 homeobox (clone 40.2D6, 1/200, Developmental Studies Hybridoma Bank, Iowa, IN, USA). After several washes with PBS, the retinas were further incubated for 1 hour at RT with Alexa-488, Alexa-568 or Texas Red conjugated secondary antibodies (Molecular Probes). They were then mounted with Vectashield mounting medium and analyzed by confocal microscopy. Positively stained cells were scored with a 40X objective on a Zeiss Axioplan fluorescence microscope, except for the TUNEL, active caspase-3 or FITC-VAD-fmk positive cells double-stained with Islet that were quantified under a 100X objective.

Immunostaining of dissociated cells

Freshly dissected or cultured retinas were mildly digested for 10 min at 37°C with Accutase (Sigma). Dissociated live cells were then fixed with 4% paraformaldehyde (w/v) in 0.1 M phosphate buffer (pH 7.4) for 1 hour at RT and washed three times with BSA in PBS (30 mg/ml, Roche). Cells corresponding to half of a retina were

cytocentrifuged on microscope slides pretreated with poly-L-lysine (Sigma). The cells were then permeated with 0.2% (w/v) Triton X-100 for 1 hour at RT and incubated overnight at 4ºC with primary antibodies against: γH2AX (1/1000); pATM (Ser^{1981}, 1/1000, Millipore); DNA-PK (1/200, Cell Signaling Technology); βIII tubulin (1/1000, TUJ-1, Covance, Paris, France); PCNA (1/250, Delta Biolabs, CA, USA); pH3 (Ser^{10}, 1/100, Millipore) or BrdU (1/1000, G3G4, Developmental Studies Hybridoma Bank). After being washed several times with PBS, the cells were incubated with Alexa-488 or Texas Red conjugated secondary antibodies for 1 h at RT. They were then mounted with Vectashield mounting medium. Positive cells were scored counting at least 10 fields under a 40X objective and photographed using a Zeiss Axioplan fluorescence microscope.

Western blotting

Individual retinas were lysed in a buffer containing 50 mM Tris-HCl (pH 6.8), 10% (v/v) glycerol, 2% (w/v) SDS, 10 mM DTT and 0.005% (w/v) bromophenol blue. The total protein from each retina was resolved on a 12% SDS-PAGE gel and the proteins were transferred to PVDF membranes (Bio-Rad, Hercules, CA, USA). The membranes were then blocked for 1 hour in TBS- or PBS-Tween 20 (0.1% w/v) containing BSA (3% w/v) and probed with antibodies against γH2AX (1/1000); H2AX (1/5000, Abcam); pChk1 (Ser^{345}); Chk1; pp70 (Thr^{389}); pAkt (Ser^{473}); Akt (all from Cell Signaling Technology and used at a 1/1000 dilution); p21 (1/100, Santa Cruz Biotechnology, Santa Cruz, CA, USA); p53 (1/500, Calbiochem); pH3 (Ser^{10}, 1/1000, Millipore); H3 (1/1000, Santa Cruz Biotechnology); βIII tubulin (1/5000, Covance); Islet1-1 homeodomain (1/200, Developmental Sudies Hybridoma Bank); Brn3a (1/100, Millipore) and β tubulin (1/10000, Sigma). The antibodies were detected with the

appropriate horseradish peroxidase-labelled secondary antibodies (Pierce, Rockford, IL, USA) and visualized with the Super Signal West Pico chemiluminescent substrate (Pierce).

RT-PCR analysis

Total RNA was extracted from freshly dissected retinas using Trizol reagent (Invitrogen) and digested with DNase I (Invitrogen). Reverse transcription was performed on 1 μg of RNA using Oligo$(dT)_{18-20}$ and the Superscript III enzyme (Invitrogen) according to the manufacturer´s instructions. Semiquantitative RT-PCR was performed using Taq polymerase (Invitrogen) under the following conditions: an initial denaturation step at 94°C for 1 min., followed by 30-35 cycles of denaturation at 94°C for 30 s, annealing at 58°C for 45 s and extension at 72°C for 45 s; and a final elongation at 72°C for 1 min. The primer sequences used were H2AX: Fw, GTCCTGCCCAACATCCAG; Rv, TGGCTCAGCTCTTTCTGTGA; p53: Fw, AGAGACCGCCGTACAGAAGA; Rv, GCATGGGCATCCTTTAACTC; ATM: Fw, CTGGATCACCCCCATCATAC; Rv, ACTGAGAGGCGTCCATGTTT; DNA-PK: Fw, GAGGCCATGATGAAAAGGAA; Rv, CGCTTTGGGGTCACTGTTAT; Ku70: Fw, CCAAAAAGCGAGTTCTGTCC; Rv, TGACGTGTCCCGTAAGTAG; Lig IV: Fw, ATGACCTGGGCTTGAAATTG; Rv, TCGTGCCACTCTTTGTCATC; and s16: Fw, TTCTGGGCAAGGAGCATT; Rv, GATGGACTGTCGGATGGCA. The RT-PCR products were visualized by ethidium bromide staining (1 μg/ml) on a 1.5% agarose gel and the identity of the products was confirmed by DNA sequencing.

Acknowledgments: This work was supported by the Ministerio de Ciencia e Innovación, Spain (Grant SAF2007–66175 to EJdlR). JB is a FPI Fellow (Ministerio de Ciencia e Innovación). We thank Dr. Violeta Gómez-Vicente for critical reading of the manuscriptreading, and Prof. Flora de Pablo for continuous encouragement and ideas. We thank Maite Seisdedos, Noemí Alvarez, Ana Robles and the staff of the CIB animal house for technical support.

Supplementary information is available at www.nature.com/cdd/

References

1. Yeo W, Gautier J. Early neural cell death: dying to become neurons. *Dev Biol* 2004; **274**(2)**:** 233-44.

2. Boya P, de la Rosa EJ. Cell death in early neural life. *Birth Defects Res C Embryo Today* 2005; **75**(4)**:** 281-93.

3. Buss RR, Sun W, Oppenheim RW. Adaptive roles of programmed cell death during nervous system development. *Annu Rev Neurosci* 2006; **29:** 1-35.

4. Kuida K, Zheng TS, Na S, Kuan C, Yang D, Karasuyama H *et al.* Decreased apoptosis in the brain and premature lethality in CPP32-deficient mice. *Nature* 1996; **384**(6607)**:** 368-72.

5. Gao Y, Sun Y, Frank KM, Dikkes P, Fujiwara Y, Seidl KJ *et al.* A critical role for DNA end-joining proteins in both lymphogenesis and neurogenesis. *Cell* 1998; **95**(7)**:** 891-902.

6. Chun J, Schatz DG. Rearranging views on neurogenesis: neuronal death in the absence of DNA end-joining proteins. *Neuron* 1999; **22**(1)**:** 7-10.

7. Orii KE, Lee Y, Kondo N, McKinnon PJ. Selective utilization of nonhomologous end-joining and homologous recombination DNA repair pathways during nervous system development. *Proc Natl Acad Sci U S A* 2006; **103**(26)**:** 10017-22.

8. Frank KM, Sekiguchi JM, Seidl KJ, Swat W, Rathbun GA, Cheng HL *et al.* Late embryonic lethality and impaired V(D)J recombination in mice lacking DNA ligase IV. *Nature* 1998; **396**(6707)**:** 173-7.

9. Gowen LC, Johnson BL, Latour AM, Sulik KK, Koller BH. Brca1 deficiency results in early embryonic lethality characterized by neuroepithelial abnormalities. *Nat Genet* 1996; **12**(2)**:** 191-4.

10. Deans B, Griffin CS, Maconochie M, Thacker J. Xrcc2 is required for genetic stability, embryonic neurogenesis and viability in mice. *Embo J* 2000; **19**(24)**:** 6675-85.

11. Biton S, Barzilai A, Shiloh Y. The neurological phenotype of ataxia-telangiectasia: solving a persistent puzzle. *DNA Repair (Amst)* 2008; **7**(7)**:** 1028-38.

12. McKinnon PJ. DNA repair deficiency and neurological disease. *Nat Rev Neurosci* 2009; **10**(2)**:** 100-12.

13. Weterings E, Chen DJ. The endless tale of non-homologous end-joining. *Cell Res* 2008; **18**(1)**:** 114-24.

14. Fernandez-Capetillo O, Lee A, Nussenzweig M, Nussenzweig A. H2AX: the histone guardian of the genome. *DNA Repair (Amst)* 2004; **3**(8-9)**:** 959-67.

15. Shiotani B, Zou L. Single-stranded DNA orchestrates an ATM-to-ATR switch at DNA breaks. *Mol Cell* 2009; **33**(5)**:** 547-58.

16. Murga M, Bunting S, Montana MF, Soria R, Mulero F, Canamero M *et al.* A mouse model of ATR-Seckel shows embryonic replicative stress and accelerated aging. *Nat Genet* 2009; **41**(8)**:** 891-8.

17. Dar I, Biton S, Shiloh Y, Barzilai A. Analysis of the ataxia telangiectasia mutated-mediated DNA damage response in murine cerebellar neurons. *J Neurosci* 2006; **26**(29)**:** 7767-74.

18. Cepko CL, Austin CP, Yang X, Alexiades M, Ezzeddine D. Cell fate determination in the vertebrate retina. *Proc Natl Acad Sci U S A* 1996; **93**(2)**:** 589-95.

19. Valenciano AI, Boya P, de la Rosa EJ. Early neural cell death: numbers and cues from the developing neuroretina. *Int J Dev Biol* 2009; **53**: 1515-28.

20. de la Rosa EJ, Diaz B, de Pablo F. Organoculture of the chick embryonic neuroretina. *Curr Top Dev Biol* 1998; **36:** 133-44.

21. Diaz B, Pimentel B, de Pablo F, de La Rosa EJ. Apoptotic cell death of proliferating neuroepithelial cells in the embryonic retina is prevented by insulin. *Eur J Neurosci* 1999; **11**(5)**:** 1624-32.

22. Valenciano AI, Corrochano S, de Pablo F, de la Villa P, de la Rosa EJ. Proinsulin/insulin is synthesized locally and prevents caspase- and cathepsin-mediated cell death in the embryonic mouse retina. *J Neurochem* 2006; **99**(2)**:** 524-36.

23. Rogakou EP, Nieves-Neira W, Boon C, Pommier Y, Bonner WM. Initiation of DNA fragmentation during apoptosis induces phosphorylation of H2AX histone at serine 139. *J Biol Chem* 2000; **275**(13)**:** 9390-5.

24. Rossi R, Lidonnici MR, Soza S, Biamonti G, Montecucco A. The dispersal of replication proteins after Etoposide treatment requires the cooperation of Nbs1 with the ataxia telangiectasia Rad3-related/Chk1 pathway. *Cancer Res* 2006; **66**(3)**:** 1675-83.

25. Tanaka T, Halicka HD, Traganos F, Seiter K, Darzynkiewicz Z. Induction of ATM activation, histone H2AX phosphorylation and apoptosis by etoposide: relation to cell cycle phase. *Cell Cycle* 2007; **6**(3)**:** 371-6.

26. Abe T, Ishiai M, Hosono Y, Yoshimura A, Tada S, Adachi N *et al.* KU70/80, DNA-PKcs, and Artemis are essential for the rapid induction of apoptosis after massive DSB formation. *Cell Signal* 2008; **20**(11)**:** 1978-85.

27. Zaugg K, Su YW, Reilly PT, Moolani Y, Cheung CC, Hakem R *et al.* Cross-talk between Chk1 and Chk2 in double-mutant thymocytes. *Proc Natl Acad Sci U S A* 2007; **104**(10)**:** 3805-10.

28. Wood A, Shilatifard A. Transcriptional blackjack with p21. *Genes Dev* 2006; **20**(6)**:** 643-7.

29. Vemuri MC, Schiller E, Naegele JR. Elevated DNA double strand breaks and apoptosis in the CNS of scid mutant mice. *Cell Death Differ* 2001; **8**(3)**:** 245-55.

30. Mayordomo R, Valenciano AI, de la Rosa EJ, Hallbook F. Generation of retinal ganglion cells is modulated by caspase-dependent programmed cell death. *Eur J Neurosci* 2003; **18**(7)**:** 1744-50.

31. Mellen MA, de la Rosa EJ, Boya P. The autophagic machinery is necessary for removal of cell corpses from the developing retinal neuroepithelium. *Cell Death Differ* 2008; **15**(8)**:** 1279-90.

32. Narasimhaiah R, Tuchman A, Lin SL, Naegele JR. Oxidative damage and defective DNA repair is linked to apoptosis of migrating neurons and progenitors during cerebral cortex development in Ku70-deficient mice. *Cereb Cortex* 2005; **15**(6)**:** 696-707.

33. Frappart PO, McKinnon PJ. Mouse models of DNA double-strand break repair and neurological disease. *DNA Repair (Amst)* 2008; **7**(7)**:** 1051-60.

34. Muotri AR, Chu VT, Marchetto MC, Deng W, Moran JV, Gage FH. Somatic mosaicism in neuronal precursor cells mediated by L1 retrotransposition. *Nature* 2005; **435**(7044)**:** 903-10.

35. Gasior SL, Wakeman TP, Xu B, Deininger PL. The human LINE-1 retrotransposon creates DNA double-strand breaks. *J Mol Biol* 2006; **357**(5)**:** 1383-93.

36. Coufal NG, Garcia-Perez JL, Peng GE, Yeo GW, Mu Y, Lovci MT *et al.* L1 retrotransposition in human neural progenitor cells. *Nature* 2009.

37. Maruyama C, Suemizu H, Tamamushi S, Kimoto S, Tamaoki N, Ohnishi Y. Genotyping the mouse severe combined immunodeficiency mutation using the polymerase chain reaction with confronting two-pair primers (PCR-CTPP). *Experimental animals / Japanese Association for Laboratory Animal Science* 2002; **51**(4)**:** 391-3.

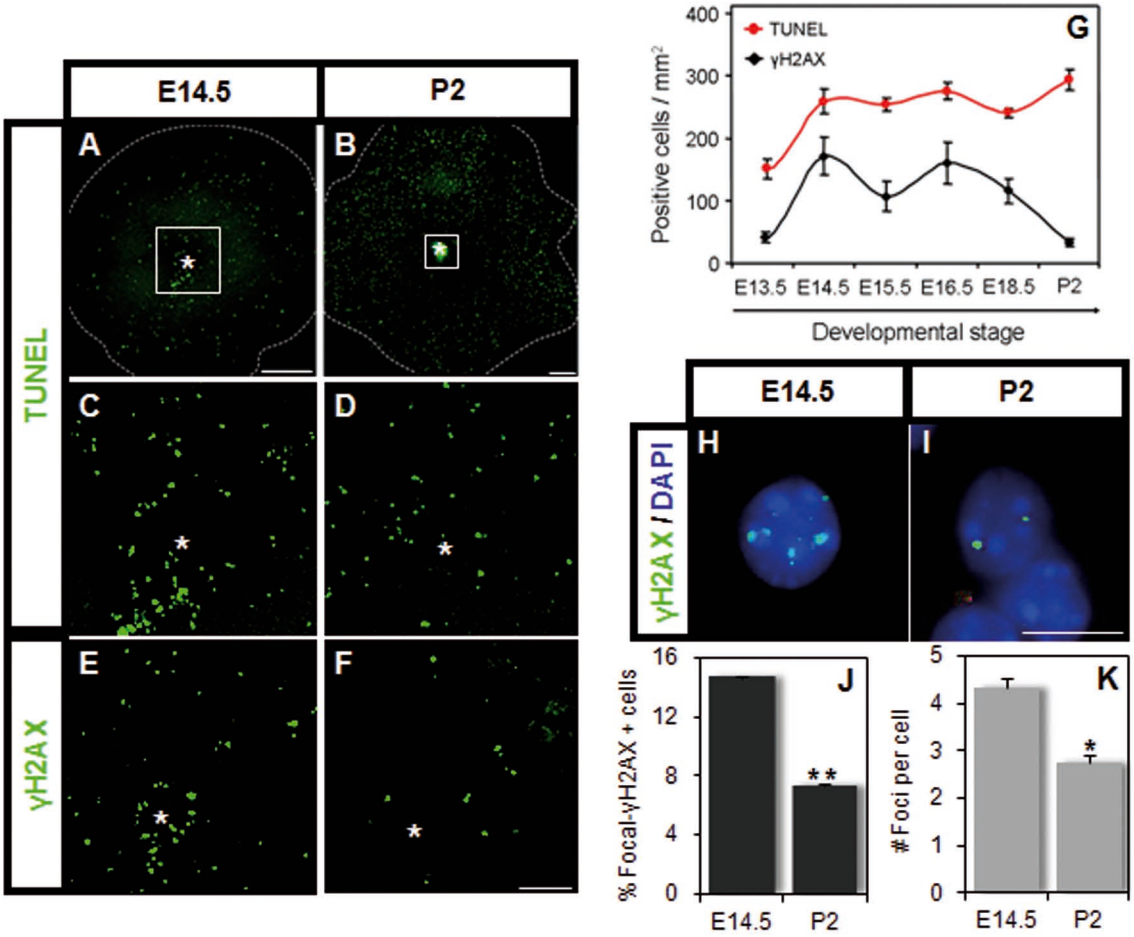
E14.5
P2
TUNEL
γH2AX
A
B
C
D
E
F
G
TUNEL
γH2AX
Positive cells / mm²
400
300
200
100
0
E13.5 E14.5 E15.5 E16.5 E18.5 P2
Developmental stage
E14.5
P2
γH2AX / DAPI
H
I
J
% Focal-γH2AX + cells
16
12
8
4
0
**
E14.5
P2
K
Foci per cell
5
4
3
2
1
0
*
E14.5
P2

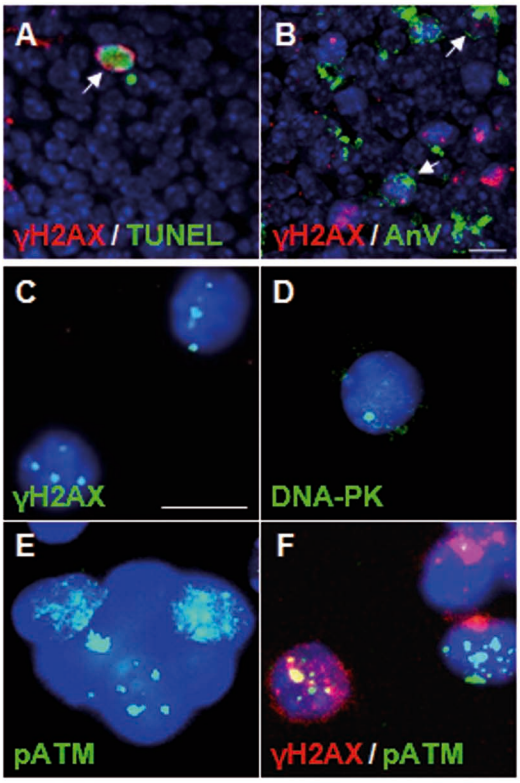
A
γH2AX / TUNEL
B
γH2AX / AnV
C
γH2AX
D
DNA-PK
E
pATM
F
γH2AX / pATM

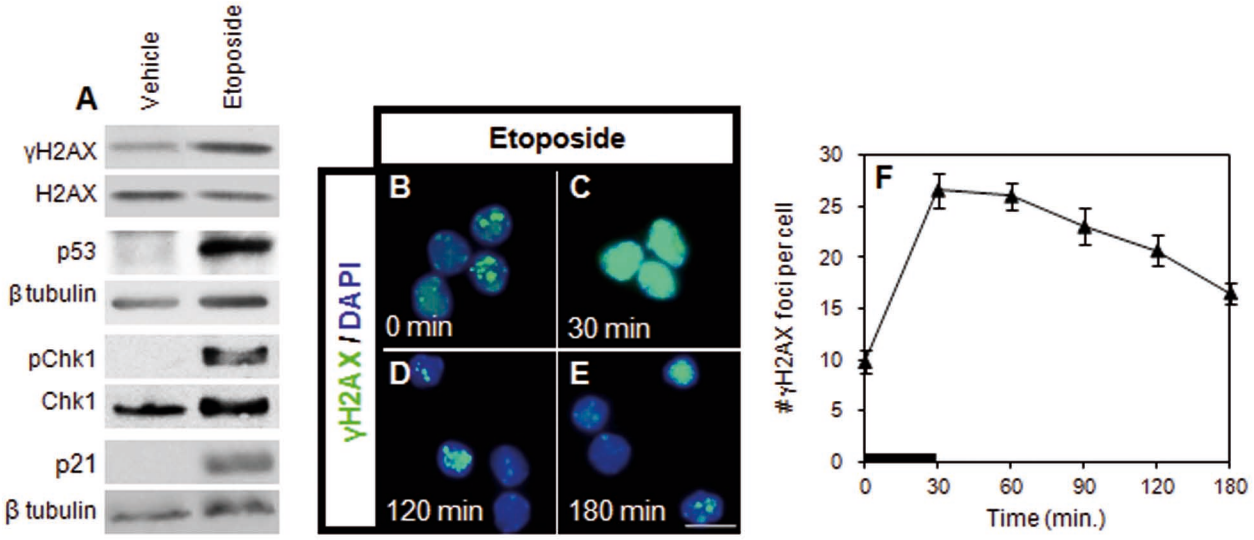
A
Vehicle
Etoposide
γH2AX
H2AX
p53
β tubulin
pChk1
Chk1
p21
β tubulin
Etoposide
γH2AX / DAPI
B
0 min
C
30 min
D
120 min
E
180 min
F
#γH2AX foci per cell
Time (min.)
0
5
10
15
20
25
30
0
30
60
90
120
180

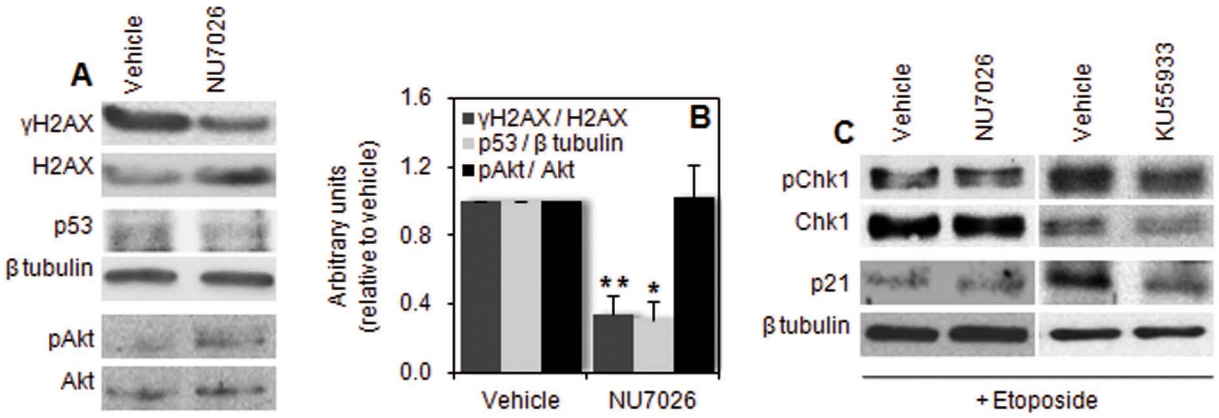
A
Vehicle
NU7026
γH2AX
H2AX
p53
β tubulin
pAkt
Akt
B
γH2AX / H2AX
p53 / β tubulin
pAkt / Akt
Arbitrary units
(relative to vehicle)
1.6
1.2
0.8
0.4
0.0
**
*
Vehicle
NU7026
C
Vehicle
NU7026
Vehicle
KU55933
pChk1
Chk1
p21
β tubulin
+ Etoposide

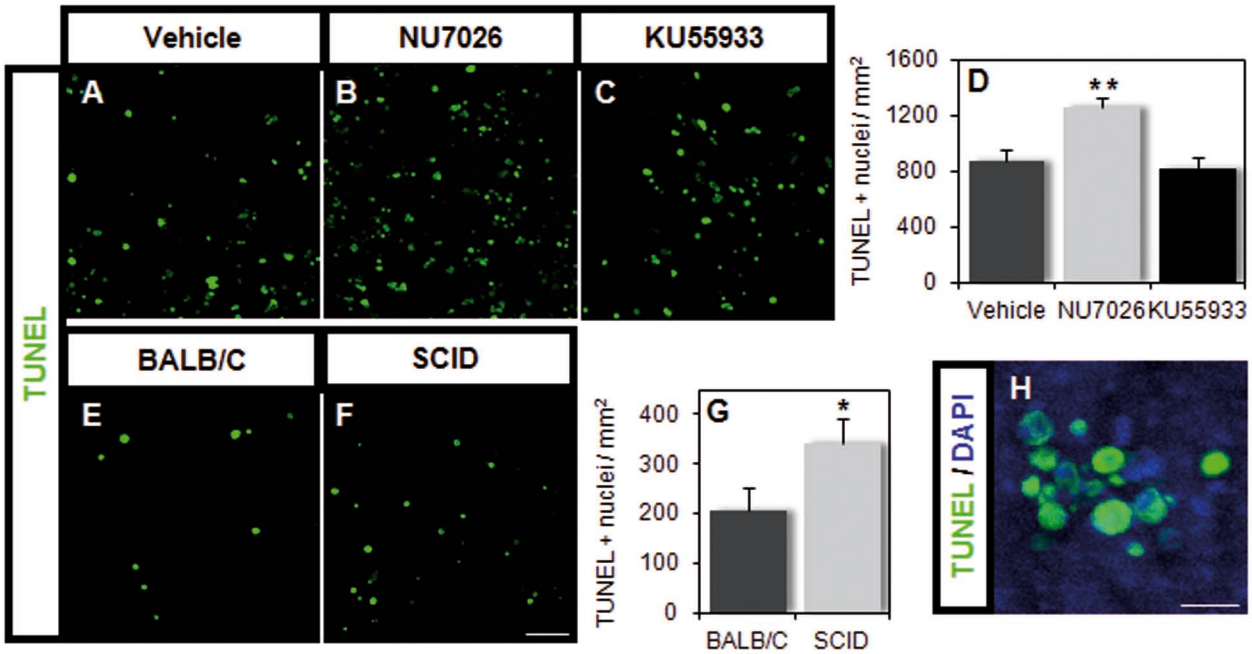
Vehicle
NU7026
KU55933
TUNEL
A
B
C
D
TUNEL + nuclei / mm²
1600
1200
800
400
0
**
Vehicle
NU7026
KU55933
BALB/C
SCID
E
F
G
TUNEL + nuclei / mm²
400
300
200
100
0
*
BALB/C
SCID
H
TUNEL / DAPI

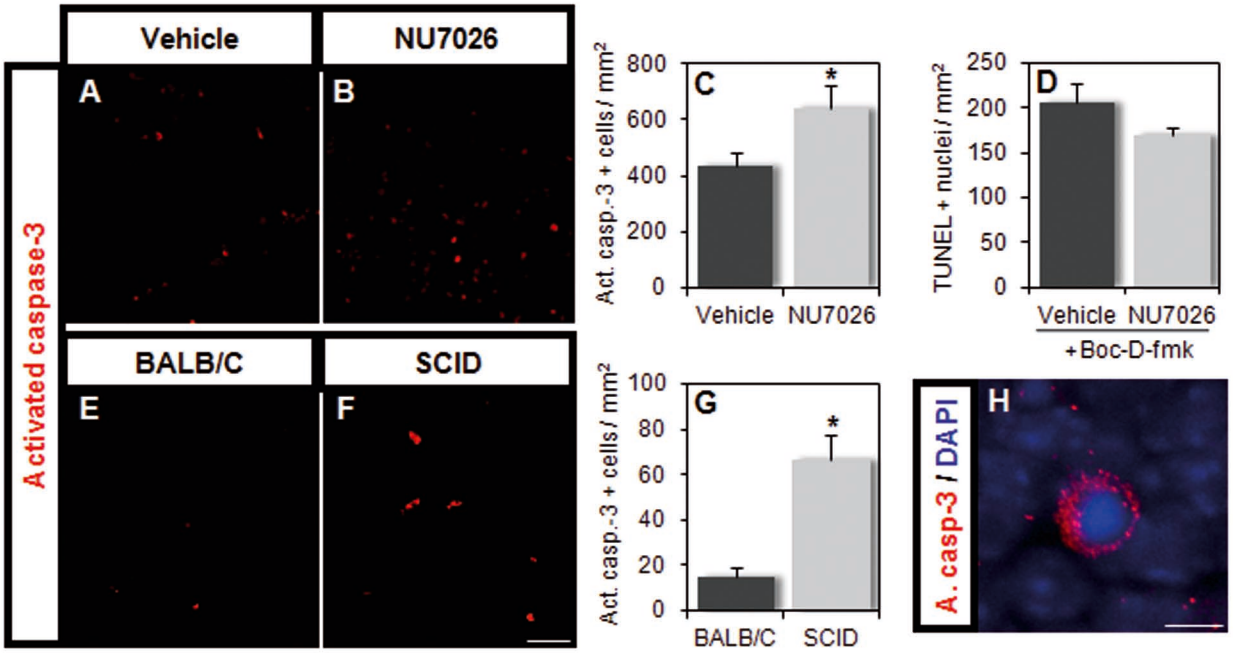
Vehicle
NU7026
A
B
Activated caspase-3
BALB/C
SCID
E
F
C
Act. casp.-3 + cells / mm²
800
600
400
200
0
Vehicle
NU7026
D
TUNEL + nuclei / mm²
250
200
150
100
50
0
Vehicle
NU7026
+Boc-D-fmk
G
Act. casp.-3 + cells / mm²
100
80
60
40
20
0
BALB/C
SCID
H
A. casp-3 / DAPI

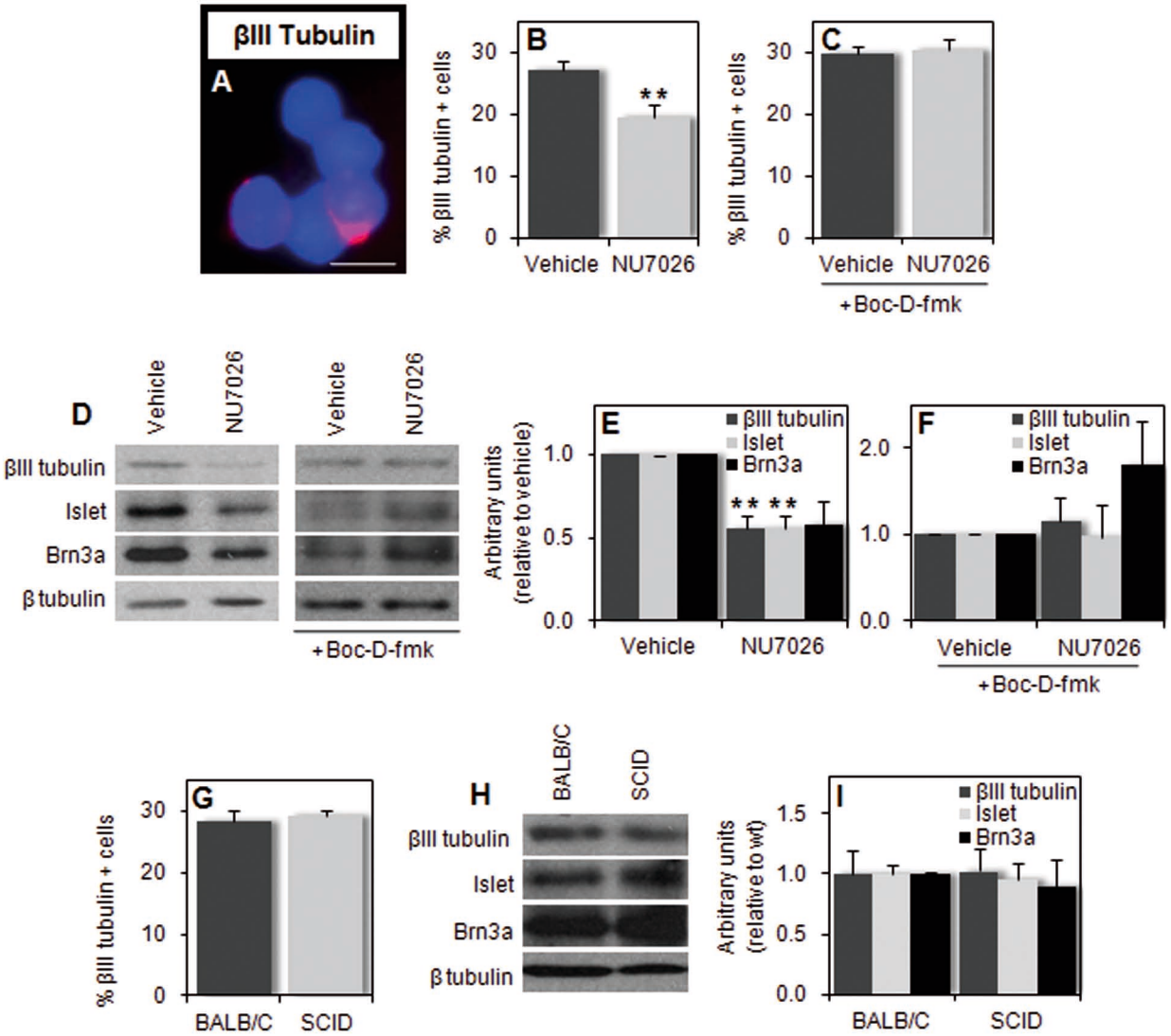
βIII Tubulin
A
B
% βIII tubulin + cells
30
20
10
0
**
Vehicle
NU7026
C
% βIII tubulin + cells
30
20
10
0
Vehicle
NU7026
+Boc-D-fmk
D
Vehicle
NU7026
Vehicle
NU7026
βIII tubulin
Islet
Brn3a
β tubulin
+Boc-D-fmk
E
Arbitrary units
(relative to vehicle)
1.0
0.5
0.0
βIII tubulin
Islet
Brn3a
** **
Vehicle
NU7026
F
2.0
1.0
0.0
βIII tubulin
Islet
Brn3a
Vehicle
NU7026
+Boc-D-fmk
G
% βIII tubulin + cells
30
20
10
0
BALB/C
SCID
H
BALB/C
SCID
βIII tubulin
Islet
Brn3a
β tubulin
I
Arbitrary units
(relative to wt)
1.5
1.0
0.5
0.0
βIII tubulin
Islet
Brn3a
BALB/C
SCID

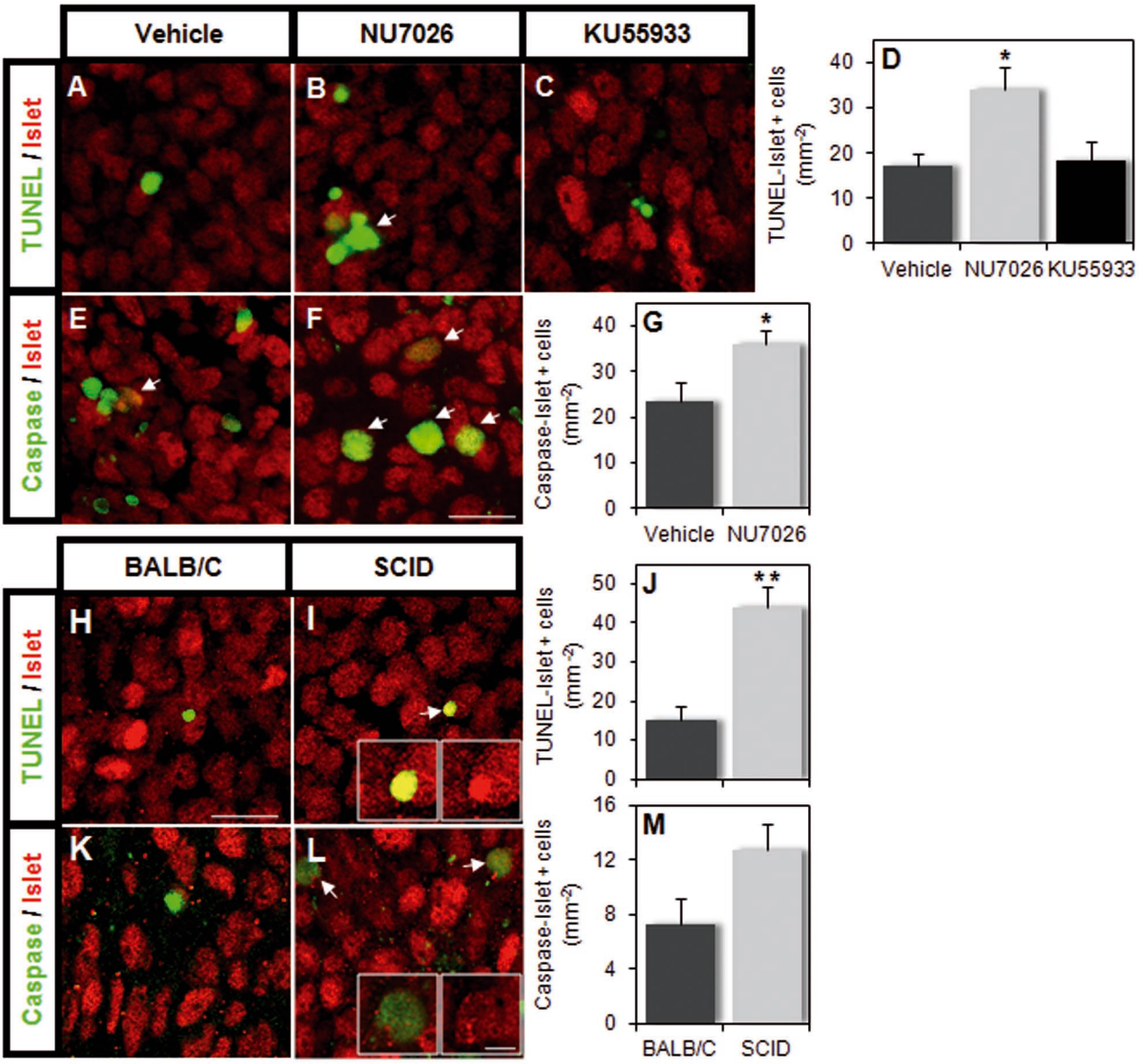
Vehicle
NU7026
KU55933
TUNEL / Islet
Caspase / Islet
A
B
C
D
E
F
G
TUNEL-Islet + cells (mm-2)
Caspase-Islet + cells (mm-2)
Vehicle
NU7026
KU55933
BALB/C
SCID
H
I
J
K
L
M
TUNEL-Islet + cells (mm-2)
Caspase-Islet + cells (mm-2)
BALB/C
SCID